

USE OF 3D PRINTING TECHNOLOGIES IN EXTERNAL RADIOTHERAPY FOR THE FABRICATION OF CUSTOMIZED BOLUS

USO DE TECNOLOGÍAS DE IMPRESIÓN 3D EN RADIOTERAPIA EXTERNA PARA LA FABRICACIÓN DE BOLUS PERSONALIZADOS

Camilo E. Pérez-Cualtán¹, Andrea Abril^{2*}, Daniel R. Suarez
Venegas³

¹ Pontificia Universidad Javeriana, School of Engineering, BASPI Research Group, Bogota, Colombia.

² Pontificia Universidad Javeriana, Facultad de Ciencias, Departamento de Física, Bogotá, Colombia.

³ Pontificia Universidad Javeriana, School of Engineering, Department of Electronic Engineering, Bogotá, Colombia.

(Received: jan./2024. Accepted: may./2024)

Abstract

Radiotherapy has challenges for irregular tumours that extend to the skin surface; thus, boluses that act as tissue compensators are used in practice. However, conventional boluses are not adapted to the patient's anatomy or lack a dosimetry characterization, decreasing their effectiveness and precision. Given this situation, this study aimed to develop a method of characterization, design, and manufacturing boluses using 3D printing to improve dose coverage in the target volume in patients with head and neck cancer in photon beams. For this, a dosimetry characterization of the 3D printing material was performed through Hounsfield Units, and a novel experimental setup was proposed to determine the depth dose profiles depending on the 3D printing parameter: infill. Subsequently, a workflow was developed to fabricate bolus through the radiotherapy plan files, and finally, the effect of a printed bolus was evaluated with an anthropomorphic phantom designed from a patient study with neck and head cancer. The dose distribution was calculated using

* andrea.j.abrilf@javeriana.edu.co

doi: <https://doi.org/10.15446/mo.n69.112586>

Monaco™ treatment planning system (TPS) based on MonteCarlo. Then the treatment was delivered onto the phantom and the dosimetric measurements were performed. The results showed that the selected 3D printing material has similar characteristics to water ($1.01 \pm 0.04 \text{ g/cm}^3$ and $-115.39 \pm 20 \text{ HU}$), making it suitable for clinical use and achieving a maximum dose of 7.8 mm with a 6 MeV beam. The ability of the workflow to generate and manufacture customized boluses adaptable to the patient's anatomy was also validated with the anthropomorphic head phantom manufactured in-house. The 95% isodose curve in the simulation was on the target volume. It can be concluded that 3D printing technologies can design and manufacture structures comparable to commercial boluses, thus eliminating the discrepancy between the planned treatment and its execution in therapy.

Keywords: bolus, 3D printing, radiation therapy, compensator tissues, CTV.

Resumen

La radioterapia presenta desafíos para los tumores irregulares que se extienden hasta la superficie de la piel; por ello, en la práctica se utilizan bolus que actúan como tejidos compensadores. Sin embargo, los bolus convencionales no se adaptan a la anatomía del paciente o carecen de caracterización dosimétrica, disminuyendo su eficacia y precisión. Ante esta situación, este estudio tiene como objetivo desarrollar un método de caracterización, diseño y fabricación de bolus mediante impresión 3D para mejorar la cobertura de dosis en el volumen objetivo en pacientes con cáncer de cabeza y cuello en haces de fotones. Para ello, se realizó una caracterización dosimétrica del material de impresión 3D mediante Unidades Hounsfield y se propuso una novedosa configuración experimental para determinar los perfiles de dosis en profundidad en función del parámetro de impresión 3D: el *infill*. Posteriormente, se desarrolló un flujo de trabajo para fabricar bolus a través de los archivos del plan de radioterapia. Finalmente, se evaluó el efecto del bolus impreso con un simulador físico antropomórfico

diseñado para un paciente con un caso de cáncer de cabeza y cuello. La distribución de dosis fue calculada usando el TPS (*treatment planning system*) MonacoTM basado en MonteCarlo, permitiendo ejecutar el tratamiento en el simulador físico como a su vez las medidas dosimétricas. Los resultados mostraron que el material de impresión 3D seleccionado tiene características similares al agua ($1,01 \pm 0,04$ g/cm³ y $-115,39 \pm 20$ HU), lo que lo hace apto para uso clínico y logra una dosis máxima de 7,8 mm con un haz de 6 MeV. La capacidad del flujo de trabajo para generar y fabricar bolus personalizados adaptables a la anatomía del paciente también se validó con un simulador físico de cabeza antropomórfico fabricado internamente. La curva de isodosis del 95 % en la simulación estaba en el volumen objetivo. Se puede concluir que las tecnologías de impresión 3D pueden ser útiles para diseñar y fabricar estructuras comparables a los bolus comerciales, eliminando así la discrepancia entre el tratamiento planificado y su ejecución en terapia.

Palabras clave: bolus, impresión 3D, radioterapia, tejido compensador, CTV.

Introduction

In MeV photon beams, the dose at the skin surface is much lower than the maximum absorbed dose, which occurs at some depth, beyond the patient's surface [1]. This area between the surface ($z = 0$ or skin) and the maximum dose D is called the build-up region, i.e., as the depth (z) increases, the electronic equilibrium conditions are reached, and the maximum dose (D_{max}) is delivered [2]. Generally, with 6 MeV photon beams from a linear accelerator (LINAC), the maximum dose is achieved at 15 mm for the skin surface [3]. Medical physicists and radiation oncologists fabricate or use boluses that act as compensating tissues to shift D_{max} and achieve the desired dose distribution to the tumour depth, since adding a tissue equivalent on the skin surface can modulate the build-up region. The boluses have a certain thickness and material

to perform their function and are placed on the patient's skin surface, aligned with the target volume. The material of these structures should be equivalent to the patient's tissue or water [4]. Some studies refer to the need for more guidance to apply a bolus correctly [1], [5] and the influence of the air-gaps on the dose deposition [6, 7]. This process is predominantly at the discretion of the radiation oncologist responsible for the treatment and the medical physicist in radiation oncology centres.

There are two types of bolus: commercial bolus as gel sheets, silicone, or thermoplastic granules. The second type is the bolus manufactured by the oncology department staff, commonly made with wet gauze or wax. The gel sheets have the disadvantage of generating air spaces when placed on the surface of the patient's skin, resulting in under-dosing of the tumour around 4% - 10% reduction over the initially planned dose [8]. At the same time, *in-situ* manufactured boluses lack characterisation in their physical properties and reproducibility [1], thus generating uncertainty about the dose deposition to the patient. Furthermore, the boluses used in therapy do not correspond faithfully to those simulated in the Treatment Planning System (TPS) [8]. The TPS bolus is designed to fit the patient's anatomy perfectly, defining an adequate thickness and volume and Hounsfield Units (HU) to deposit the maximum dose in the tumour.

As another concept, three-dimensional (3D) printing technology allows the fabrication of complex volumetric objects of virtually any geometry with various materials. Applying this type of technology in ontological surgical planning and radiotherapy has shown benefits in manufacturing complex boluses that are specific and personalised for each patient [9–11]. Diaz-Merchan et al. studied the interaction of electron beams with 3D printed materials, using Monte Carlo simulations and experimental measurements to evaluate boluses' uniformity and dosimetric characteristics [12]. Meanwhile, Malone et al. conducted a retrospective study on the fit quality of 3D printed boluses at various treatment sites, concluding their suitability, especially in head, neck, scalp and extremity regions [6].

However, current approaches have not focused on establishing a validated methodology or workflow so that the use of 3D printed boluses can be standardised in clinical practice since many processing parameters of the 3D printed parts may have dosimetric effects on the patient, and most have just worked with electron beams [12]. A limitation arises when simulating a radiotherapy plan with an externally designed bolus, requiring bolus fabrication, additional CT scans, and plan revisions, leading to workflow disruptions. The main objective of this study is to develop a workflow for bolus design and fabrication using 3D printing technologies. This workflow aims to generate structures from the radiotherapy plan to deliver the appropriate dose to tumors targeted by photon beams. This is significant because current work has been primarily focused on electron beams, and there is a need for specific applications when using bolus in photon beam external radiotherapy. This will be achieved through the characterization of 3D printing parameters and pre-clinical evaluation.

Materials and Methods

A complete workflow has been proposed to design and manufacture personalised boluses, ensuring that the generated structures are characterised by 3D printing material. The first stage involves meticulously characterising the 3D printing material, particularly the main parameter, infill. This parameter plays a critical role in achieving the desired clinical target volume (CTV) depth, as well as flexibility and thickness, providing a comfortable solution as close as possible to the physical configuration. The selection of a suitable 3D printing material for physical and dosimetric characterisation with 6 MeV photon beams further demonstrates the thoroughness of this process. The proposed workflow considers several variables in the operation of oncology units, highlighting its adaptability and reliability. The performance in a pre-clinical environment with an anthropomorphic head phantom using the treatment planning system based on Monte-Carlo dose deposition calculation on the patient, Monaco™, is performed by Elekta. The plan's evaluation is

contrasted by delivering the treatment and using specific dosimetric measurements, such as film dosimetry. The results provide a quantifiable result employing the proposed workflow in the selected pathology.

Material Characterisation

This work is performed using the FDM (Fused Deposition Modeling) 3D printing technologies due to their practicality, cost, variety of materials, and recent applications in oncology and radiotherapy. Due to its physical and manufacturing characteristics, the 3D printing material selected was Thermoplastic Polyurethane (TPU). The main characteristic of TPU is its high flexibility, softness to the touch, unlike other rigid printing materials, and density like different biological tissues [4]. This material will also be in contact with the patient's skin, so comfort in these processes is essential. The use of infill percentage was utilised to describe the properties of the bolus material, which is a parameter that had been previously investigated in rigid thermoplastics [13]. The material was characterised by manufacturing specimens at different infill percentages (Table 1). We used an FF-STD 3D printer (FusedForm, Colombia) and the TPU material from a standard manufacturer (Wanhuachemica, China).

Initially, the printed part's physical density for the three infills was determined. Measurements of dimensions (width, length, and thickness) and mass were made using a digital balance with a precision of 0.01 g and a manual calibrator. To determine the Hounsfield Units (HU), a computed tomography (CT) scan was performed at the Centro Oncológico Javeriano of the Hospital Universitario San Ignacio in Bogotá (Table 1). The CT scan was taken while the specimens were in direct contact with the surface of the treatment couch coated with solid water to avoid noise in the images.

3D Printing Parameter	Value
3D printed specimen's dimensions	6 x 6 x 1 cm
Number of 3D printed specimens	21
Infill of 3D printed specimens	7 with 30%, 7 with 70%, 7 with 100%
CT Scan Parameter	Value
Peak voltage	120 kV
3D Printing Parameter	Value
Slice thickness	2.0 mm
Field of view	19.8 cm

TABLE 1. *Parameters of 3D printing specimens characterisation and CT Scan*

Subsequently, the Depth Dose Profiles (PDD) samples were determined with a 6 MeV photon beam. A solid water block configuration was implemented to obtain the dosimetric characterisation data. Printed TPU specimens were placed on the solid water blocks and irradiated with a field photon beam at a source-to-surface distance (SSD) of 100 cm from the Elekta Precise™ Treatment System linear accelerator. For the procedure, the SSD was always kept constant at the surface of the specimens, as seen in Figure 1. In each measurement, the LINAC table was moved one (1) cm upwards, and a specimen of one (1) cm was also removed to maintain the SSD. 200 Monitor Units (MU) of the LINAC and a maximum rate of 339 MU/min were used. A calibrated Farmer-type ionisation chamber was used to measure the dose, which was immersed in the block of solid water with the specimens, to determine the PDD curves corresponding to each fill and type of material.

Finally, due to the experimental configuration shown in Figure 1, the three infills of PDD were at the same depth, so a bi-exponential type equation for each experimental arrangement (infill 100%, 70%, and 30%) was used to fit the data to determine the of each infill. The depth at which the maximum dose was produced was determined through an optimisation algorithm, as shown in Table 2.

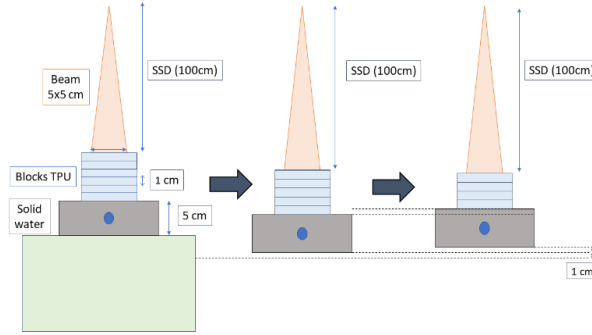


FIGURE 1. *Experimental linear accelerator (LINAC) configuration for dosimetric characterisation of specimens 3D printed on TPU material*

The form of the bi-exponential type equation describing the PDDs is shown in equation 1, where A , a , B , b , and C are constants.

$$D_{max}(x) = A \exp^{-ax} + B \exp^{-bx} + C \quad (1)$$

Design and Manufacturing Workflow

A structured workflow was established through collaboration with medical physicists to address the inconsistency between the bolus outlined in the Treatment Planning System (TPS) and the standard bolus utilised in therapy. This workflow outlines two approaches for the manufacturing and design process using 3D printing, ensuring the creation of a personalised bolus tailored to the patient's anatomy, regardless of the chosen method. Derived from the framework proposed by the authors in [12, 13] and depicted in Figure 2, the first method involves starting with the existing bolus generated in the radiation therapy plan by the medical physics department. The present work presents a methodology where the bolus structure from the plan is exported as a stereolithography file (STL), separated from other structures, and exported with a uniform infill determined by the Medical Physicist based on Hounsfield Units (HU). Since these files often have suboptimal quality, post-processing steps are necessary to refine the 3D virtual bolus, including re-meshing and mesh fixing, while maintaining the

integrity of the anatomical fit. The fit is verified by examining the contours of the bolus STL file in CT axial slices. Alternatively, the second method proposes a variable infill bolus design, which may be requested by the medical physics department or deemed necessary to deposit the maximum dose at a specific depth for clinical interest. The method provides an optimal 3D printing infill determined for each anatomical point based on the Clinical Target Volume (CTV) depth in the CT image, ensuring maximum dose deposition at desired points as per Equation 3.

$$\text{Infill}_{opt} = \min(D_{max}i - \text{depth}_{CTV}) \quad (2)$$

$$D_{max} = \sum_{i=1}^N D_{max} \quad (3)$$

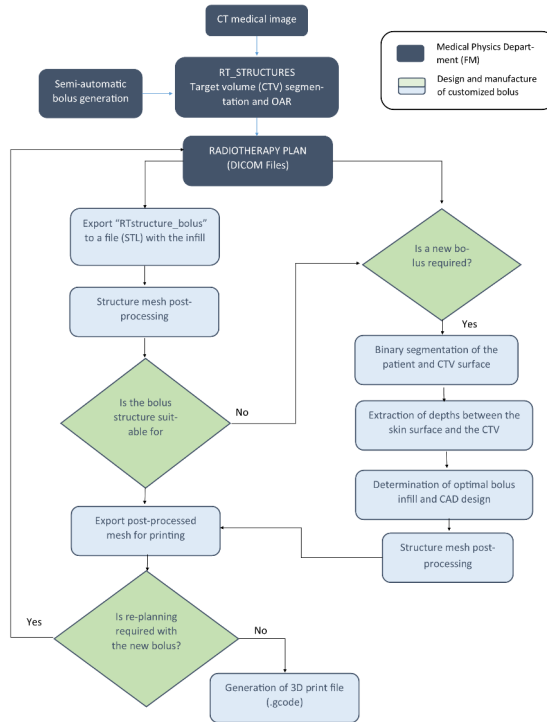


FIGURE 2. *Proposed workflow for design and fabrication of customized 3D printed bolus from radiotherapy plan*

Pre-clinical Evaluation

Finally, the aim was to evaluate the effect of including a customised 3D-printed bolus versus a traditional flat uniform bolus in a pre-clinical environment. For this purpose, an anthropomorphic head phantom (see Figure 3) was designed and fabricated from a dataset HN-CHUS-018 of the Cancer Imaging Archive repository (<https://www.cancerimagingarchive.net/>). The dataset of a 57-year-old male patient with a tumour in the larynx (primary site) stage III was selected. DICOM series was used to segment the body surface, taking into account the HU of the body fat in the 3D Slicer software, where the slice thickness of the images was 1.17 mm. The segmentation was exported to an STL format to divide the phantom into different pieces and to manufacture it with 3D printing.

In the same way, it was designed couplings and the space to place the detector (dosimetric film), as shown in Figure 3, to perform the dosimetric test after dose calculation and treatment delivery. The 3D printing material used was PLA (polylactic acid), with an infill of 10%, providing a 0.3 g/cm^3 density. The target volume was defined as a region on the anthropomorphic phantom of a human head.

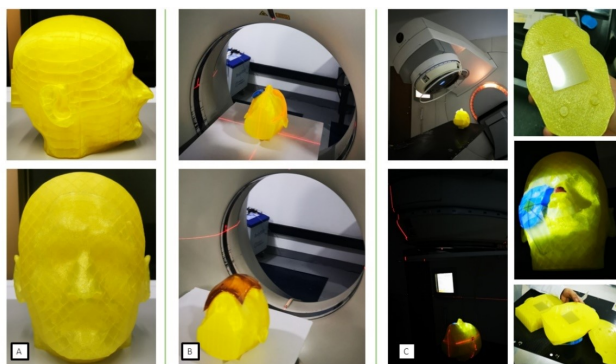


FIGURE 3. 3D printed anthropomorphic head phantom (A) Frontal and sagittal view of 3D printed anthropomorphic phantom (B) CT scan of the patient with printed bolus (top) and commercial uniform flat bolus (bottom) and (C) Dosimetric evaluation of 3D printed bolus.

Pre-calibrated gafchromic EBT3 radiochromic film (<https://www.ashland.com/>) was used as a detector, which was cut to 5×5 cm to match the cross-sectional contour of the phantom with a pre-exposure density equal to 0.17 du, sensitivity comparable to 0.68 du and uniformity of 1.27%. The sensitometric curve was determined during calibration, and a maximum difference of 2.3% was obtained. The curve presented a quadratic adjustment with an $r^2 = 99.95\%$, with coefficients $a = 21.71$ and $b = 2.88$. Three films from the same batch were located between the phantom cuts at three depths (5, 10, and 15 cm), and one test film on the skin surface (Figure 3C). The LINAC Elekta Precise™ Treatment System was used, with the gantry positioned at 325.1° to deliver 400 MU using a 6 MeV beam of 10×10 cm field size in the frontal direction towards the bolus. They were then scanned to determine the film dose, calibrated with LINAC in Sun Nuclear software (<https://www.sunnuclear.com/>). The results are valuable for evaluating the differences between the Monte-Carlo calculation performed with the TPS and the delivered treatment.

Results

Material Characterisation

Initially, the physical density of the material was determined at different infills. For the 100% infill, a density of 1.015 ± 0.04 g/cm³ was calculated; for the 70% infill, it was 0.697 ± 0.001 g/cm³, and for the 30% infill, it was 0.413 ± 0.025 g/cm³. Linear regression was performed to determine the density of other infills to cover the entire range, with physical density as the dependent variable and infill as the independent variable. The regression model results showed a confidence statistic and a mean square error, as shown in Table 2. The nominal physical density of the TPU material was determined by the manufacturer (<https://en.whchem.com/>).

After the physical density, HU was determined through CT scanning of the 3D printed specimens of the TPU material, as shown in Figure 3b. The scanned image was processed, and each

infill's mean and standard deviation were obtained as follows: 100% infill: -115.39 ± 19.53 HU, 70% infill: -414.35 ± 29.81 HU, and 30% infill -731.71 ± 26.79 HU. Also, like validation, air HU was calculated (-988.07 ± 19.70). Similarly, a linear regression was performed to cover the entire infill range. The dependent variable was the mean HU, and the independent variable was the infill. The regression model results showed a confidence statistic of $R^2 = 90\%$ and a mean square error of 67.65. The electron density was determined to complete the material's physical characterisation. For this, the equation proposed by [14] was used, which was determined to calibrate the relative electron density of CT scanners for radiotherapy treatment planning.

Infill Percentage (%)	Physical density (g/cm³)	Electronic Density	Hounsfield Units (HU)	Dmax (mm)
30	0.41	0.27	-731.71	14.70
40	0.48	0.35	-654.02	14.24
50	0.56	0.43	-566.44	13.28
60	0.65	0.52	-478.87	12.32
70	0.69	0.58	-414.35	12.54
80	0.82	0.69	-303.72	10.40
90	0.91	0.78	-216.14	9.44
100	1.01	0.88	-115.39	7.80

TABLE 2. *Physical and dosimetric properties of the 3D printed TPU samples at different infill percentages*

The data points were fitted to a bi-exponential type equation for each experimental arrangement (Infill 100%, 70%, and 30%) with a R^2 more significant than Figure 4. The uncertainty associated with the procedure was calculated considering the physical principle of attenuation through its percentage difference. The percentage dose attenuation of each material was determined through Equation 1 by simulating the attenuation curves with the data obtained from physical density and data from the NIST platform, XCOM (NIST, 2021). At the NIST database, the chemical composition of the material and water was input in a range of energies from 1-10 MeV

to simulate the attenuation coefficient. For a 100% TPU infill, the uncertainty is 0.86%; for a 70% infill, it is 6.89%; and for the 30% infill, the uncertainty is 8.47% in the measurements.

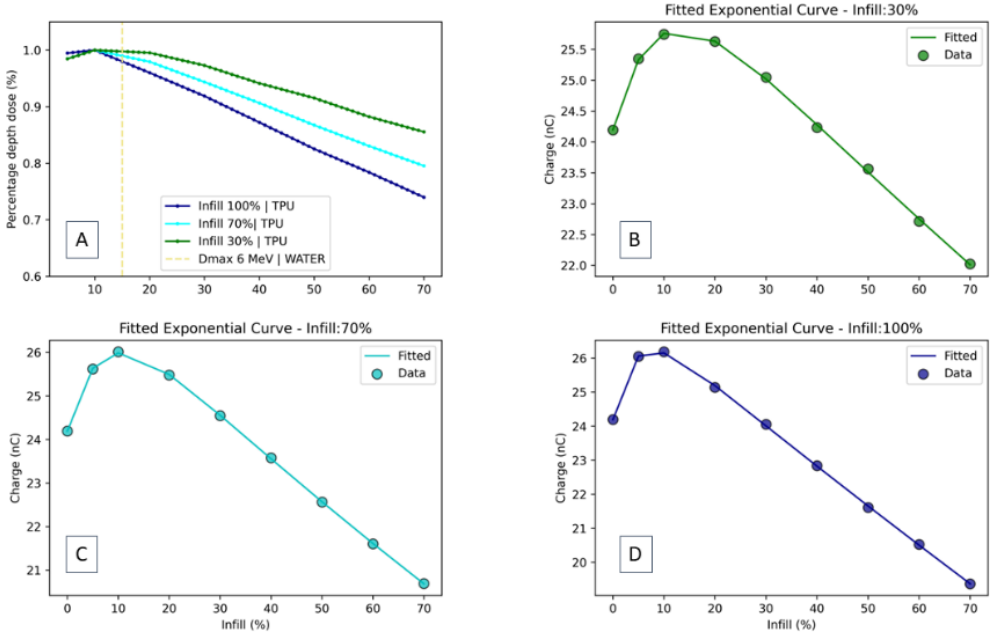


FIGURE 4. PDD of the 3D printed TPU samples with (A) the proposed experimental setup for three different infills and the water PDD as a reference, (B) bi-exponential fit to PDD data for the 30% infill, (C) bi-exponential fit to PDD data for the 70% and (D) bi-exponential fit to PDD data for the 100%

Design and Manufacturing Morkflow

Initially, the results of method 1 of the proposed workflow were evaluated, in which the bolus file generated in the RT structure folder was exported from the radiotherapy plan, and the raw file and the post-processed file were compared, as shown in Figure 5. The bolus exported directly from the unprocessed radiotherapy plan required a fabrication time of 3 hours and 32 minutes and 10.99 meters of material, while the post-processed bolus required a fabrication time of 2 hours and 26 minutes and 9.62 meters of material. Similarly, the thickness measurements of the CAD model

were compared with the printed models, presenting a difference of 4.2% for the unprocessed bolus and 1.3% for the post-processed bolus. These boluses were manufactured with a random infill since, through method one, the medical physicist determines the appropriate HU corresponding to a specific infill, as shown in the characterisation of the material.

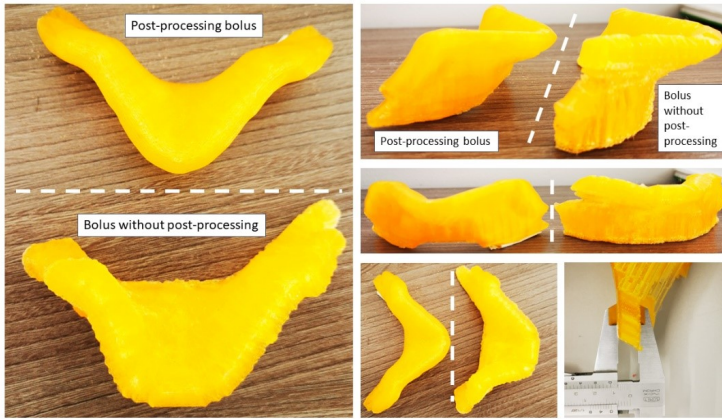


FIGURE 5. *Bolus printouts from method one workflow. Post-processed Bolus vs. Bolus without post-processing from case radiotherapy plan HN-CHUS-025 from Cancer Imaging Archive Database*

Regarding method 2 of the workflow, the algorithm implemented to measure the Euclidean distances (depths) from the skin surface to the tumor or CTV was validated. For this, a single volume slice of two Cancer Imaging Archive datasets (HN-CHUS-025 and HN-CHUS-034) was taken for proof-of-concept validation with the algorithm generated in Python © and the 3D Slicer © software (<https://www.slicer.org/>) as the gold standard. Using the Euclidean distances or depths at which the CTV was located, the optimal infill at each point was determined using Equation 1. An infill map was generated, which was used to design the bolus with a variable infill (see Figure 6). The bolus with variable infill required a fabrication time of 4 hours, 16 minutes, and 12.23 meters of material.

For either method, it is possible to perform replanning with the new bolus structure generated in the TPS without the need

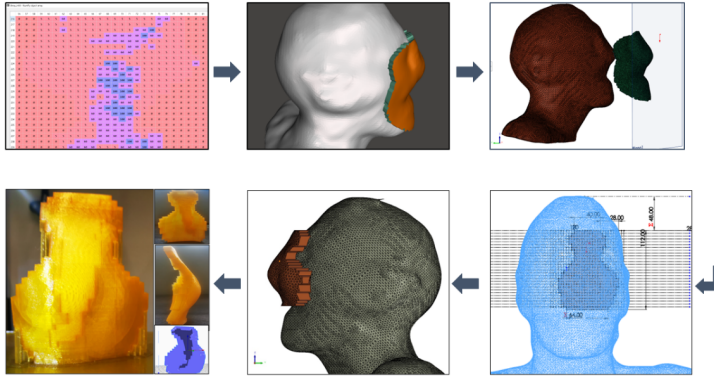


FIGURE 6. *Generation of the customized bolus from method 2 of the proposed workflow. Infill map, bolus CAD design, and 3D printed bolus from case radiotherapy plan HN-CHUS-025 from Cancer Imaging Archive Database*

to perform a second CT scan with the bolus; in fact, this characteristic of the proposed methodology shows the adaptability to the clinical routine in the radiation oncology departments. For replanning, both the medical images of the patient and the bolus structure are imported into an image processing software such as 3D Slicer ©(<https://www.slicer.org/>), and the bolus STL file will import the contours to be loaded to the 2D slices of the images. This procedure was validated in the dosimetric research software Primo (<https://primoproject.net/primo/>), successfully importing the bolus structure and the CT images, where the bolus file had the anatomical fit coordinates to the patient, so it is possible to simulate with a virtual bolus and with physical and dosimetric characteristics set by the user without the need to perform another scan.

Pre-clinical Evaluation

CT scans showed the anatomic fit of the 3D printed bolus compared to a flat uniform bolus conventionally used in therapy. No air gaps are generated with the 3D-printed bolus because the bolus was designed from the patient's anatomy through medical imaging. While the flat bolus was placed in the face region, simulating a

clinical setting, even though it was attached with adhesive tape to the patient, it generated air gaps, which were quantified similarly to results presented in [15]. Figure 7A shows the dose distribution in the anthropomorphic head phantom for the highest infill bolus (density: 1.015 g/cm^3). As it passes through the 3D-printed bolus, the dose passes through 1 cm of additional tissue, electronic equilibrium occurs, and the maximum dose is deposited. The 95% isodose curves are continuously found on the phantom's skin surface compared to the 100% dose.

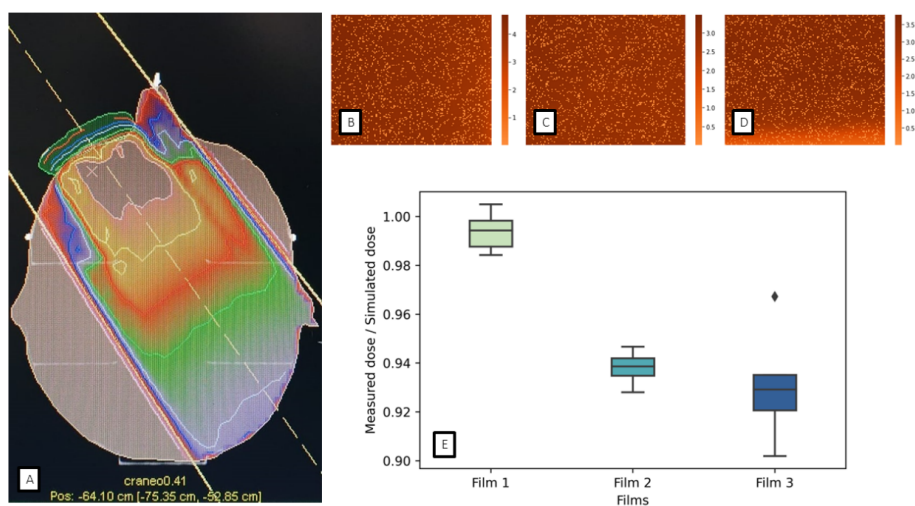


FIGURE 7. Dose distribution in the anthropomorphic head phantom. (A) Calculated by Monaco Treatment System with the 3D printed bolus and scanned EBT3 films. (B) Film 1 is located 5 cm from the surface in the sagittal axis (C) Film 2 is located 10 cm from the surface in the sagittal axis, (D) Film 3 is located 15 cm from the surface in the sagittal axis, and (E) Relationship between measured and simulated dose

After demonstrating that the 3D-printed bolus could provide an adequate surface dose under dose calculation performed with MonacoTM, we proceeded to dose measurement with the calibrated EBT3 films. The average dose recorded by the film on the surface between the bolus and the patient was $3.438 \pm 0.029 \text{ Gy}$, the dose on the shallower film was $4.288 \pm 0.008 \text{ Gy}$, the dose recorded on the intermediate film was 3.573 ± 0.006 , and the dose determined on the deeper film recorded a value of $3.058 \pm 0.015 \text{ Gy}$. The measured experimental values were contrasted with the simulated values in

the TPS, as shown in Figure 7E. The ratio between experimental and simulated values was within 10% statistical variability.

Discussion

Commercially available clinical tools currently used in radiation therapy are typically based on traditional manufacturing processes, often resulting in non-compliant geometries, slow manufacturing processes, and high costs. In this project, we evaluated a 3D printing material (TPU) that had yet to be extensively studied and the influence of the variability of the infill or filling of the bolus to modify the maximum dose at specific depths. It should also be clarified that this project's scope focused on tumours that extend to the skin's surface, which are treated with photon beams, and that optimal control is not possible at specific depths due to the physics of the electronic balance of particles. It is required to have it at shallower depths. The beam selection of 6 MeV photon beam is related to the treatment protocol implemented for pathologies that fulfil the characteristics described before and located in the head and neck for the dosimetric characterisation and experimental tests [16, 17], where tumours are on the surface, and great depths could be dose restrictive.

The standard deviations determined for the three infills (30%, 70%, and 100%) are around 25 HU, and none exceeded 30 HU, so it can be stated that the fabricated pieces had an adequate uniform density. The infill with the lowest standard deviation was 100% infill, an expected result because it did not include air spaces in its interior. Likewise, the HU of the air in the CT scan was close to -1000 with a standard deviation of ± 19.70 . The results were similar to those presented by Michiels *et al.*[18], who determined -127 ± 29 HU for TPU material at 100% infill, while in the present study, we determined for 100% infill, -115.39 ± 19.53 HU. As the infill of the parts increases, the HU tends to zero. Therefore, we can also state that there may be slight variations depending on the 3D printing material and 3D printing parameters used to fabricate the parts [16]. Also, physical density plays a vital role in radiotherapy as it is

used for different tests and calibrations. The material characterized by a 100% infill presented a density of $1.015 \pm 0.04 \text{ g/cm}^3$, similar to distilled water; this suggests that TPU could be used as a water equivalent material without needing a depth correction factor.

Another main objective of this project was to demonstrate, in a clinical way, that the build-up region can be modulated through the 3D printing parameters, as shown in Table 2, the results of the experimental PDD tests. For a 100% infill, the D_{max} is 7.8 mm, a value lower than that achieved without 6 MeV bolus beams (approximately 15 mm), so exciting applications could be found in clinical practice. The D_{max} in PDD curves in Figure 4 do not show a variation for the three infills; this was due to the experimental setup, in which each 1 cm specimen of TPU was removed the linear accelerator stretcher was moved 1 cm down. Finally, by finding the respective equations that fit the data using an optimization algorithm, it was possible to find the D_{max} for each infill, similar to previous studies with other materials [13, 18].

It should be noted that fabrication times can increase significantly if no post-processing is done to the bolus structure and even more so if larger volume boluses, such as a breast bolus, need to be fabricated, as shown in the workflow results. Compared to how the STL bolus file is directly exported to print, we can still determine air gaps with a printed bolus. So, it can be reconfirmed that a post-processing process is necessary for the structures. For the present study designing a bolus from the images and post-processing, the CAD file eliminates the air gaps, although this also depends on the medical images.

For method 2 of the workflow, an algorithm was proposed to measure the depth at which the tumor is located to select the appropriate 3D printing infill, allowing the D_{max} . The proposed algorithm worked correctly in determining the depths of the tumors in the proof of concept, where two datasets of radiotherapy plans were tested. However, some processes of method two could be automated to reduce the time of the bolus structure generation. This alternative had not been previously explored in the literature,

so it may be of great interest for medical physicists to test it, as it could make the work of bolus addition in therapy more efficient. Similarly, previous studies showed only one path for bolus fabrication. They did not allow re-planning with the generated bolus's CAD file, while a complementary perspective is given with the proposed workflow. Either of the two methods proposed in the diagram in Figure 2 has a customized and personalized bolus.

The anthropomorphic head phantom print was an exploratory option to evaluate the effect of including a 3D-printed bolus in a pre-clinical context. The internal density does not resemble the density of the skull tissue but that of the lung. However, this option was explored to evaluate the geometric distribution of the dose calculated by the TPS through the Monte Carlo calculation compared to the dosimetric measurement. The simulation's 95% isodose curve is found on the skin surface, as shown in Figure 7. According to the literature, this value would be reached at 1.5 cm from the surface without the bolus, so it could be stated that the printed bolus had a good effect. A limitation of 3D printed bolus fabrication is that of printing time. Mainly, the material used for bolus fabrication (TPU) requires very low printing speeds, although a water-like density was achieved with a 100% infill, an aspect that could justify its implementation. Likewise, in terms of its economical implementation, its use could be feasible, contributing to personalised medicine and the cost of a flat commercial bolus.

Conclusions

3D printing technologies and their parameters make it possible to modulate the maximum dose deposition at a given depth. With the results obtained, the patient does not need to undergo more than one CT scan, ensuring a perfect fit to the body surface by performing the simulations with the determined HU and PDD. The density or HU of the designed bolus can be selected to maximise the surface coverage of the tumour, and the bolus could be manufactured with the infill according to the calibration curves. Also, a bolus with variable infill could be manufactured if different points of maximal dose deposition are required to be modulated.

Although studies on the relationship between 3D printing and bolus manufacturing have been reported in the literature, this project explored options that could significantly impact the workflow of medical physics departments.

Acknowledgments

Special thanks to the Medical Physics team at the Centro de Oncología Javeriano-Hospital Universitario San Ignacio for permitting us to introduce the radiotherapy workflow and discuss the context of implementing a solution for the usual routines. Thanks also to the Hospital Universitario del Valle Medical Physicist team for permitting us to understand the daily routine where the bolus is involved and the technical challenges related to it.

References

- [1] V. Vyas and et al., *Medical Dosimetry* **38**, 268 (2013).
- [2] T. Aoyama and et al., *Med. Phys.* **47**, 6103 (2020).
- [3] X. Liu and et al., *Oncol. Res. Treat.* **43**, 140 (2020).
- [4] M. Alssabbagh and et al., *Int. j. adv. appl. sci.* **4**, 168 (2017).
- [5] T. Kawamoto, N. Shikama, and et al., *BMC Cancer* **21**, 109 (2021).
- [6] C. Malone, E. Gill, and et al., *J. Appl. Clin. Med. Phys.* **23**, e13490 (2022).
- [7] A. Kassaeia, P. Blocha, and et al., *Med. Dosim.* **25**, 127 (2000).
- [8] S. Y. Park, C. H. Choi, and et al., *PLoS One* **11**, e0168063 (2016).
- [9] R. A. Canters and et al., *Radiother. Oncol.* **121**, 148 (2016).
- [10] Y. Zhao and et al., *Med. Dosim.* **42**, 150 (2017).
- [11] G. Dipasquale, A. Poirier, and et al., *Radiat. Oncol.* **13**, 203 (2018).

- [12] J. Diaz-Merchan, C. Español-Castro, and et al., Appl. Radiat. Isot. **199**, 110908 (2023).
- [13] R. Ricotti and et al., Phys. Med. **39**, 25 (2017).
- [14] S. J. Thomas, Br. J. Radiol. **72**, 781 (1999).
- [15] J. L. Robar and et al., Pract. Radiat. Oncol. **8**, 221 (2018).
- [16] Q. Ma, M. Rejab, and et al., Proc. Inst. Mech. Eng. C J. Mech. Eng. Sci. **235**, 4254 (2020).
- [17] K. Dibs, E. Gogineni, and et al., Cancers **16**, 688 (2024).
- [18] S. Michiels and et al., Radiother. Oncol. **128**, 161 (2018).
- [19] B. A. Dyer, D. Campos, and et al., Phys. Med. **77**, 138 (2020).
- [20] G. C. Baltz and et al., J. Appl. Clin. Med. Phys. **20**, 89 (2019).
- [21] A. Karl, *The Production of Custom Bolus using 3D printers for applications in Radiation Therapy. Master Thesis* (University of Canterbury, 2016).
- [22] K. Bahhous, M. Zerfaoui, and et al., Journal of Radiotherapy in Practice **20**, 210 (2020).